Biochimica et Biophysica Acta 1797 (2010) 476–486

Contents lists available at ScienceDirect

Biochimica et Biophysica Acta

journal homepage: www.elsevier.com/locate/bbabio

Mitochondrial metabolism during fasting-induced daily torpor in mice

Jason C.L. Brown *, James F. Staples

Department of Biology, University of Western Ontario, London, Ontario, Canada N6A 3K7

ARTICLE INFO

Article history:
Received 16 September 2009
Received in revised form 6 January 2010
Accepted 11 January 2010
Available online 18 January 2010

Keywords:
Liver
Fasting
Calorie restriction
Proton leak
Top-down regulatory analysis

ABSTRACT

During fasting, mice (*Mus musculus*) undergo daily bouts of torpor, considerably reducing body temperature (T_b) and metabolic rate (MR). We examined females of different laboratory strains (Balb/c, C57/6N, and CD1) to determine whether liver mitochondrial metabolism is actively reduced during torpor. In all strains, we found that state 3 (phosphorylating) respiration rate measured at 37 °C was reduced up to 35% during torpor for at least one of the substrates (glutamate and succinate) used to fuel respiration. The extent of this suppression varied and was correlated with T_b at sampling. This suggests that, at the biochemical level, the transition to and from a hypometabolic torpid state is gradual. In fasted non-torpid animals, T_b and MR still fluctuated greatly: T_b dropped by as much as 4 °C and MR was reduced up to 25% compared to fed controls. Changes in T_b and MR in fasted, non-torpid animals were correlated with changes in mitochondrial state 3 respiration rate measured at 37 °C. This suggests that fasting mice may conserve energy even when not torpid by occasionally reducing T_b and mitochondrial oxidative capacity to reduce MR. Furthermore, proton conductance was higher in torpid compared to non-torpid animals when measured at 15 °C (the lower limit of torpid T_b). This pattern is similar to that reported previously for daily torpor in *Phodopus sungorus*.

1. Introduction

On average, house mice (*Mus musculus*) weighing approximately 25 g have less than 10 g of body fat [1]. During fasting—even between foraging bouts—these fat stores are rapidly depleted [2,3]. Therefore, house mice might be expected to invoke physiological energy-saving mechanisms when fasted in order to reduce energy expenditure. Many small endotherms, including house mice [4], employ daily torpor—a suppression of metabolic rate (MR) to as low as 30% of basal MR (BMR) for a period of several hours [5]—during times of actual or predicted food shortage. Because MR is suppressed, body temperature (T_b) usually also declines during daily torpor, to as low as 15 °C [6]. How MR suppression is achieved during daily torpor has been debated for several decades [5,7,8] and was one focus of this study.

As much as 90% of whole-organism oxygen consumption takes place in the mitochondria [9]; therefore, the reduction of MR during daily torpor likely reflects a reduction in mitochondrial respiration rate in various tissues. There had been no studies of mitochondrial metabolism during daily torpor until we examined it in the dwarf Siberian hamster (*Phodopus sungorus*) [10]. We found that liver mitochondrial state 3 (phosphorylating) respiration rate was reduced by 30–70% during torpor (compared to normothermic levels) when measured in vitro at 37 °C. This reduction was solely due to a decreased capacity for substrate oxidation, likely upstream of electron transport chain (ETC) complex III. Changes in ADP phosphorylation, such as phosphate transport, adenine nucleotide transport, and ATP synthesis, were not involved, although ATP-consuming processes are known to be actively downregulated during torpor in this species [11]. Furthermore, we demonstrated increased inner mitochondrial membrane (IMM) proton conductance during torpor, which offset the decreased substrate oxidation such that state 4 respiration rate was not reduced during torpor [10]. This was an unexpected observation given predictions that decreased mitochondrial proton conductance could conserve energy in hypometabolic states [12].

The changes in mitochondrial metabolism that occur during daily torpor are likely one of the end results of upstream signaling cascades that are triggered by environmental and/or endogenous cues. Dwarf Siberian hamsters undergo daily torpor spontaneously when acclimated to short days, even while being fed ad libitum at thermoneutral temperatures [13,14]. Therefore, photoperiod is thought to be the dominant cue for spontaneous torpor induction in *Phodopus*, and increased production of melatonin by the pineal gland is necessary for torpor to occur [15, but see also 16]. Testosterone [17], prolactin [18], and leptin [19] levels must also be low to allow spontaneous torpor in this species, but none of these latter signals is sufficient to induce spontaneous torpor independently. By contrast, house mice readily enter torpor when fasted for as little as 12 h, with only moderate (<20%) loss of body mass [20]. Fasting-induced torpor occurs regardless of the photoperiodic conditions, although photoperiod can influence the depth and duration of fasting-induced torpor [21]. The molecular mechanisms that regulate fasting-induced torpor in mice are partially known, and roles for the sympathetic nervous

* Corresponding author. Tel.: +1 519 661 2111x80166; fax: +1 519 661 3935.
E-mail address: jbrow63@uwo.ca (J.C.L. Brown).

0005-2728/$ – see front matter © 2010 Elsevier B.V. All rights reserved.
doi:10.1016/j.bbabio.2010.01.009

system, leptin, ghrelin, and neuropeptide Y (NPY), among others, have been proposed [22]. Although moderate food restriction can increase the frequency of spontaneous torpor bouts in short-day acclimated hamsters [23], they do not undergo fasting-induced daily torpor in long-days until they have lost considerable (>25%) body mass [24], if at all [25]. Therefore, both the environmental stimulus and the signaling pathways involved in bringing about spontaneous daily torpor in *P. sungorus* and fasting-induced daily torpor in house mice are different, despite some overlapping elements, and this gives us reason to suspect that the changes in mitochondrial metabolism that occur during torpor may also differ between these two species. For this reason, in this study, we examined liver mitochondrial metabolism in torpid and non-torpid house mice, and we have compared the results obtained here to our previous work [10].

Our data suggest that mitochondrial respiration is suppressed during fasting-induced daily torpor in mice, and the mechanisms involved differ from *P. sungorus*, but also differ among the three mouse strains studied. Also, as seen in *P. sungorus*, liver mitochondria had higher IMM proton conductance when measured at torpid temperatures (15 °C), suggesting that increased proton leakiness may be a fundamental feature of daily torpor. Finally, fasting occasionally decreased mitochondrial oxidative capacity in non-torpid animals—an unexpected result seen only in animals with moderately lowered T_b and MR—which may allow for some additional energy savings in fasted animals without the large decreases in T_b associated with torpor.

2. Materials and methods

2.1. Animals

This project was approved by the local Animal Use Subcommittee and conformed to the guidelines of the Canadian Council on Animal Care. Three strains (Balb/c, CD1, and C57/6N) of female mice were examined in this study, and all animals were obtained from Charles River Laboratories (Saint-Constant, Quebec, Canada). Animals were 2–3 months old upon arrival. Animals were housed individually in cages (30×12×12 cm) filled with Beta Chips for bedding and provided with two 2-inch nesting squares (Ancare), which they readily converted to nests. Animals were housed at 20±1 °C, 12 h light/12 h dark and were given 1 week to acclimate to these conditions before surgical procedures were carried out to implant temperature telemeters (see next section). Animals were allowed 2 weeks to recover from their surgical procedure before sampling began, and all animals of a given strain were sampled within 3 months of the first animal sampled. Non-torpid and torpid animals were sampled randomly throughout this period. Animals were provided with food and water ad libitum. Balb/c and CD1 mice were split into two groups and fed different diets: one group was fed standard rodent chow (Prolab RMH 3000 5P00, LabDiet), and the other group was fed a high-linoleic acid diet (5.5 mg g^{-1} diet, TestDiets). Dietary polyunsaturated fatty acid (PUFA) content has been shown to affect hibernation patterns [26] and mitochondrial metabolism in hibernators [27], and short-day acclimated *P. sungorus* have been shown to prefer diets rich in PUFA [28]. However, diet had no significant effect on any parameter examined in this study and data from the two diet groups were combined. C57/6N mice were only fed standard rodent chow.

2.2. Measurement of T_b and MR

Body temperature was measured using telemetry as previously reported for dwarf Siberian hamsters [10]. Metabolic rate was measured using flow-through respirometry as previously reported for thirteen-lined ground squirrels [29], except that flow rates through the Plexiglas containers were 100–200 ml min^{-1}.

2.3. Experimental protocol

Two hours prior to the onset of darkness, animals were transferred from their cages to the Plexiglas chamber for simultaneous measurement of MR and T_b. Water was provided ad libitum, but there was no food in the chamber. In our study, we considered animals torpid when T_b had been less than 31 °C for at least 30 consecutive minutes, based on a previous definition [6], and T_b was not increasing, to ensure that animals arousing from torpor were not sampled. Animals were considered non-torpid when T_b had been greater than 31 °C for at least 30 consecutive minutes, and T_b was not declining. Daily torpor usually occurred for the first time about 12 h after food was removed, and then occurred again 24 and 48 h after the first bout. Fasting was never permitted to exceed 72 h. Torpid animals used in this study were sampled during the second day's bout, which would be enough time for them to acclimate to the respirometry chamber, and non-torpid controls were sampled following this bout, while still being fasted.

2.4. Mitochondrial isolation and measurement of respiration rate and membrane potential

Non-torpid animals were killed by anesthetic overdose, as required by animal care protocols, whereas torpid animals were killed by cervical dislocation (to prevent initiation of arousal), as previously described [10]. The liver was removed and immediately transferred to ice-cold homogenization buffer [10]. The anesthetic used does not affect mitochondrial properties [30]. Mitochondria were isolated as described elsewhere [10].

Mitochondrial respiration rates were measured using temperature-controlled polarographic O_2 meters, and mitochondrial membrane potential ($\Delta\Psi_m$) was measured using tetraphenylphosphonium (TPP^+), a lipophilic cation whose uptake by mitochondria is $\Delta\Psi_m$-dependent. Both procedures have been described previously [10]. We did not measure mitochondrial matrix volume because it has been shown that changes in this parameter have little effect on measurements of $\Delta\Psi_m$ when using TPP^+ [31]. As in our previous study of torpor in *P. sungorus*, we did not use nigericin to eliminate ΔpH in our assays. Nigericin can inhibit mitochondrial respiration rate, even with succinate as substrate [32], and can reduce mitochondrial respiratory control ratios [33]. Its omission is unlikely to affect our results as ΔpH is not the dominant component of the proton motive force in mitochondria. Moreover, ΔpH changes little with temperature [34] or between experimental conditions shown to alter mitochondrial respiration [35,36]. Kinetics of the components of oxidative phosphorylation (substrate oxidation, ADP phosphorylation, and proton leak) were measured using succinate in the presence of rotenone. Values for succinate-driven respiration rates were taken from the kinetic curves (i.e., state 3 was taken from the phosphorylation kinetic curve, and state 4 was taken from the proton leak kinetic curve). Glutamate respiration (in the presence of malate) was measured in a separate assay, as described elsewhere [10].

2.5. Data analysis

Differences between non-torpid and torpid animals were assessed using a generalized linear model using strain and metabolic state (non-torpid or torpid) as the factors in the analysis. To determine the effects of T_b on mitochondrial respiration rate, non-torpid and torpid animals were analyzed independently with a generalized linear model using strain as a factor and T_b as a covariate. Non-significant interactions were always dropped from the model statement. These data analyses were performed using SAS 9.0.

Kinetic curves were fitted to equations as described previously [10]. Differences in the kinetics of the components of oxidative phosphorylation were determined using top-down regulatory

analysis. This approach requires pairwise comparisons between a control state and an effect state. In our study, kinetic comparisons were made between i) non-torpid (control state) and torpid (effect state) animals, and ii) non-torpid animals sampled at a T_b of ≥36.5 °C (control state) and all other non-torpid animals (T_b < 36.5, effect state). Kinetic differences were determined by a Monte-Carlo approach based in part on Ainscow and Brand [37]. Microsoft Excel 2003 was used for this analysis. For each pairwise comparison (control vs. effect) for a particular component of oxidative phosphorylation, we calculated an integrated elasticity (IE) value [38], which represents the proportional change in mitochondrial respiration rate that the change in kinetics of that component would have brought about if the component were to have had complete control over respiration rate. We then generated 500 simulated data sets (with sample sizes equal to the experimental data set) in which the control state data was simulated via normally-distributed random number generation corrected for the experimental control state mean and standard error, and the effect state was simulated via normally-distributed random number generation corrected for the experimental control state mean, the effect state standard error, and the IE value. For each simulated data set, we determined the mean simulated respiration rate value for the control and effect state. The *P*-values reported for kinetic differences reflect the proportion of simulated data sets that show a difference between the control and effect data set in the same direction as the IE value. For example, a *P*-value of 0.01 indicates that simulated control and effect mean values were different in the same direction as the IE value for 99% of the simulated data sets.

3. Results

A preliminary experiment characterized fasting-induced torpor in Balb/c mice. When fed, animals had a high and relatively constant T_b, and daily torpor was never observed. Fasting caused T_b to fluctuate more compared with fed mice, and resulted in the occurrence of daily torpor, with T_b dropping by as much as 15 °C, to values just above ambient temperature. Torpor occurred as early as 7.5 h after fasting began, and mice typically underwent one (or more) bouts of torpor each day of the fast, which never exceeded 72 h (Table 1). Animals usually entered torpor during the scotophase and aroused either just before or just after the photophase began (Fig. 1A). This temporal pattern allowed us to distinguish daily torpor from hypothermia, the latter being characterized by the apparent inability to spontaneously arouse without assistance (i.e., in our case, being refed). Mice that became hypothermic saw their T_b begin to decline during the photophase, and did not show any signs of arousal even after nearly 24 h (Fig. 1B). At this point, they were refed in order to prevent death. These hypothermic mice were not sampled in this study.

When sampled on the second day of a fast, T_b of torpid animals was about 10 °C lower than that of non-torpid animals, and MR was nearly 70% lower (Table 2). There was no significant interaction between mouse strain and metabolic state for either MR or T_b, suggesting that any differences among strains in mitochondrial properties during torpor cannot be explained by differences in the level of whole-animal metabolic suppression at sampling. Within all three strains, fasted non-torpid and torpid animals did not differ in terms of body mass (either before or after fasting), daily rate of relative body mass loss during fasting, or liver mass (Table 2). Therefore, fasted animals sampled when not torpid responded to fasting in the same way as those animals sampled when torpid, and the effect of torpor on mitochondrial properties cannot be explained by differential responses to fasting between the groups. Furthermore, the rate of body mass loss observed in fasted animals in our study is comparable to the rates seen in previous studies [39]. Because non-torpid animals were sampled following their torpor bout, fasting duration tended to be longer for normothermic animals, but the difference was only significant for Balb/c mice (Table 2). We subsequently examined our Balb/c mitochondrial data for effects of fasting duration, but we found that no parameter examined was significantly influenced.

Table 1
Torpor characteristics of fasted mice. A selection of Balb/c mice (N = 18) were fasted for 72 h (but not sampled for mitochondrial isolation for this study) in each of two separate weeks in order to characterize daily torpor in this species. Body temperature (T_b), but not metabolic rate, was monitored throughout the bout.

	Mean	Standard error	Maximum	Minimum
Time spent torpid T_b < 32 °C (hours)	28.0	2.9	48.3	8.9
Bout length (hours)	5.6	0.4	7.9	2.6
Minimum T_b (°C)	22.6	0.3	25.3	21.6
Time to first bout after initiation of fasting (hours)	13.3	2.0	38.1	7.4
Number of bouts per day	1.7	0.2	3.0	0.8

When measured in vitro at 37 °C, state 3 respiration rate using glutamate/malate was reduced in torpid animals, particularly in CD1 and C57/6N, by up to 34% (Fig. 2A). For succinate, there was a significant interaction between strain and metabolic state: state 3 respiration rate was reduced during torpor by 35% and 22% in Balb/c and C57/6N, respectively, but was 17% higher in CD1 during torpor (Fig. 2B). State 4 respiration rate was not reduced during torpor in any strain using either substrate (data not shown).

Mitochondrial respiration rate is the result of the activity of the components of oxidative phosphorylation that control it. State 3 respiration rate is determined by the activity of both the substrate oxidation component (i.e., substrate transporters, TCA cycle, and mitochondrial electron transport chain) and the ADP phosphorylation component (i.e., ANT, phosphate transporter, ATP synthase). State 4 respiration rate is determined by the activity of both the substrate oxidation component and the proton leakiness component. In turn, the activity of any component of oxidative phosphorylation is determined by its capacity and the value of $\Delta\Psi_m$. Differences in the capacity of a particular component of oxidative phosphorylation between two states can be determined by comparing levels of activity at the same value of $\Delta\Psi_m$ as determined by kinetic analysis. We compared the kinetics of substrate oxidation, ADP phosphorylation, and proton leak at 37 °C for all strains between torpid and non-torpid animals using succinate-driven respiration to determine whether there were changes in the capacity of any components. Substrate oxidation capacity differed between non-torpid and torpid animals only in Balb/c, where it was reduced during torpor at membrane potential values near state 3 but was increased during torpor at membrane potential values near state 4 (Fig. 3). ADP phosphorylation capacity was reduced during torpor in both Balb/c and C57/6N but was increased in CD1 (Fig. 4). IMM proton leakiness was reduced during torpor only in Balb/c mice (Fig. 5).

In this study, animals were sampled when either non-torpid or torpid according to established criteria (see Section 2). The T_b of non-torpid animals at the time of sampling, however, ranged from 33.9 °C to 37.6 °C, and for torpid animals this range was 21.5 °C to 30.5 °C. These changes in T_b were correlated with changes in MR (non-torpid: r^2 = 0.34, P = 0.03; torpid: r^2 = 0.30, P = 0.03). We therefore examined the effect of T_b at sampling on mitochondrial respiration rate measured in vitro at 37 °C. There was no effect of T_b on state 4 respiration regardless of substrate (data not shown). Glutamate-driven state 3 respiration tended to decrease as T_b declined in non-torpid animals, although this was not statistically significant (Fig. 6A). During torpor, glutamate-driven respiration was negatively correlated with T_b (Fig. 6B). Succinate-driven respiration correlated significantly with T_b for both non-torpid and torpid animals: for non-torpid animals, the correlation was positive and linear (Fig. 6C), whereas in torpor, the correlation was quadratic, and mitochondrial respiration rate was lowest in animals with T_b near 25 °C at sampling (Fig. 6D).

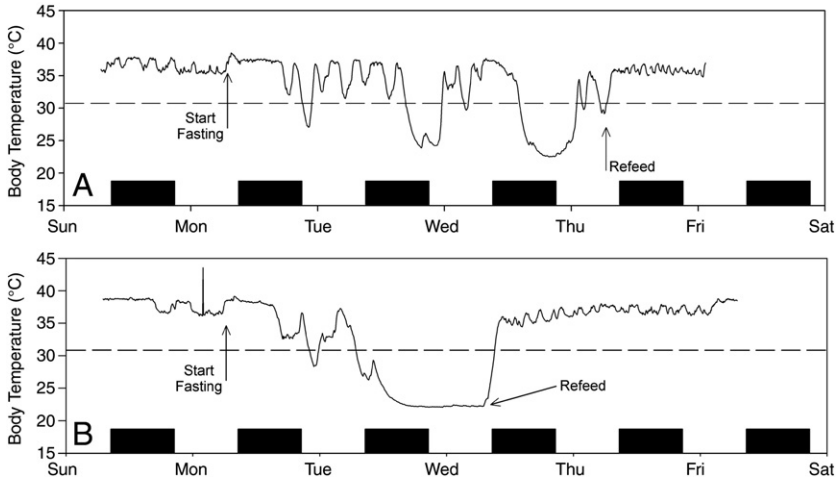

Fig. 1. Daily torpor in mice, and its distinction from hypothermia. Body temperature (T_b) of two individual Balb/c mice over the course of a week during which fasting occurred. Photophase began at 9 pm EST, and scotophase (black bars) began at 9 am EST. Fasting began just prior to the start of the scotophase on Monday (7 am) and ended 3 days later. Prior to fasting, mice maintained a relatively constant T_b and torpor was not observed. Once fasting began, T_b became more variable, and bouts of daily torpor occurred, where T_b dropped below 31 °C (indicated by dashed line) for more than 30 consecutive minutes. A. This mouse underwent one or more bouts of daily torpor on each of the 3 days of fasting. B. This mouse underwent a bout of daily torpor on the first day, but become hypothermic on the second day and only aroused after having been refed. For both mice, once food was returned, T_b stabilized near 37 °C, and no bouts of torpor were observed.

The same trends were observed when MR was correlated to mitochondrial respiration rate, but the correlations were weaker, and only the relationship between MR and succinate-driven state 3 respiration rate in non-torpid mice approached significance ($P = 0.07$; data not shown).

In order to analyze the effects of T_b on the kinetics of the oxidative phosphorylation components in non-torpid animals, it was necessary to bin T_b into discrete 1 °C intervals. Compared to animals with T_b near 37 °C, the ADP phosphorylation component was suppressed in animals with T_b near 36 °C, 35 °C, or 34 °C, whereas substrate oxidation was suppressed only in animals with T_b near 36 °C or 35 °C, though it tended to be lower at 34 °C as well (Fig. 7A). For torpid animals, we binned T_b into discrete 2 °C intervals and examined only the two strains that had shown active regulated inhibition of mitochondrial state 3 respiration rate during daily torpor (Balb/c and C57/6N). For torpid Balb/c mice, our kinetic analysis showed that when sampled with a T_b near 26 °C, there was suppression of substrate oxidation, and at T_b near 24 °C, both substrate oxidation and ADP phosphorylation were suppressed (Fig. 7B). IMM proton leakiness was reduced in torpid animals at all T_b values examined (data not shown). For torpid C57/6N animals, the phosphorylation component was suppressed in animals sampled at T_b near 22–26 °C, whereas substrate oxidation was only suppressed in animals with T_b near 24 °C, and had higher activity in animals with T_b near 22 °C (Fig. 7C). In neither strain was either component of oxidative phosphorylation significantly inhibited in non-torpid animals sampled at 28 °C, nor were any animals in these strains sampled at higher T_b.

We also examined the effect of in vitro assay temperature on mitochondrial metabolism in Balb/c mice. While succinate-driven state 3 and state 4 respiration rates were significantly lower when measured at 15 °C in both non-torpid and torpid animals, there was no effect of metabolic state on either state 3 or state 4 respiration rate (data not shown). In contrast state 3 had been significantly lower in torpid Balb/c animals when measured at 37 °C (Fig. 2B). Although state 4 respiration rate did not differ between non-torpid and torpid animals when measured at 15 °C, IMM proton leakiness was significantly higher in torpid mitochondria compared to non-torpid mitochondria at this temperature. As a result, proton leakiness in mitochondria from torpid animals measured at 15 °C was not significantly different from mitochondria from non-torpid animals when measured at 37 °C (Fig. 8).

4. Discussion

4.1. Mitochondrial respiration is actively suppressed during daily torpor in fasted mice

Our data show that mitochondrial respiration rate is actively suppressed during fasting-induced daily torpor in mice. Each mouse strain showed reduced mitochondrial state 3 respiration rate with at least one of the two substrates used to fuel respiration in this study. Compared with *P. sungorus* the extent of suppression of glutamate-driven respiration rate was lower in mice, but succinate-driven state 3 respiration rate was suppressed to a similar extent [10]. The mechanisms responsible for this suppression differed both inter-specifically (i.e., between mice and *P. sungorus*) and intraspecifically (i.e., among the three strains of mice).

Table 2
Whole-animal measurements of animals sampled in this study. Within any column, values with different letters are significantly different ($P < 0.05$) by two-way ANOVA followed by Tukey's post-hoc test. Percentage values were arcsine transformed prior to statistical analysis.

Strain	Metabolic state	Body mass before fast (g)	Body mass after fast (at sampling) (g)	Liver mass after fast (at sampling) (g)	Body mass lost during fast (% of body mass before fast day^{-1})	Body temperature at sampling (°C)	Metabolic rate at sampling (mL O_2 h^{-1} g^{-1})	Fasting duralion at sampling (hours)
Belb/c	Non-torpid	30.2 ± 1.38 ac	27.4 ± 1.32 a	1.10 ± 0.06 a	10.0 ± 0.82 a	35.9 ± 0.31 a	3.2 ± 0.21 a	43.5 ± 0.67 a
	Torpid	28.1 ± 0.99 ac	26.4 ± 1.34 a	1.07 ± 0.06 a	12.4 ± 1.19 a	25.6 ± 0.58 b	15 ± 0.28 b	37.9 ± 1.4 b
CD1	Non-torpid	34.4 ± 0.95 b	28.7 ± 0.6 a	0.96 ± 0.05 a	10.3 ± 0.87 a	36.8 ± 0.44 a	3.0 ± 0.44 a	3.86 ± 0.75 b
	Torpid	37.1 ± 0.95 b	29.2 ± 0.82 a	1.06 ± 0.05 a	11.5 ± 1.19 a	26.4 ± 1.01 b	1.1 ± 0.18 b	38.8 ± 0.79 b
C57	Non-torpid	25.0 c	22.2 ± 1.16 b	0.84 ± 0.04 b	13.0 a	35.8 ± 0.77 a	2.7 ± 0.51 a	37.2 ± 1.55 b
	Torpid	26.8 ± 1.56 c	20.9 ± 0.70 b	0.74 ± 0.05 b	11.1 ± 1.25 a	24.4 ± 0.67 b	0.85 ± 0.20 b	3.54 ± 0.72 b

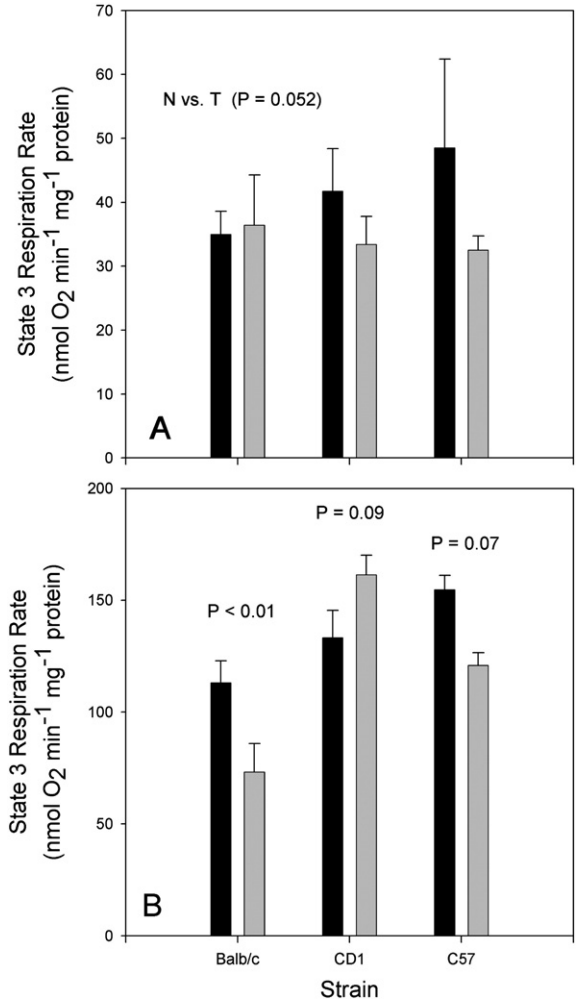

Fig. 2. Liver mitochondrial state 3 respiration rate measured in vitro at 37 °C. A. Glutamate/malate-fueled respiration rate was reduced in torpid animals (grey bars) compared to non-torpid animals (black bars). B. Succinate-fueled respiration (in the presence of rotenone to prevent reverse electron transport) was reduced in Balb/c and C57/6N mice and increased in CD1 mice. Data are means ± SEM. For glutamate respiration, $N = 7/5$ (normothermic/torpid) for Balb/c, $N = 9/11$ for CD1, $N = 4/6$ for C57/6N. For succinate respiration, $N = 8/8$ for Balb/c, $N = 9/12$ for CD1, $N = 4/7$ for C57/6N.

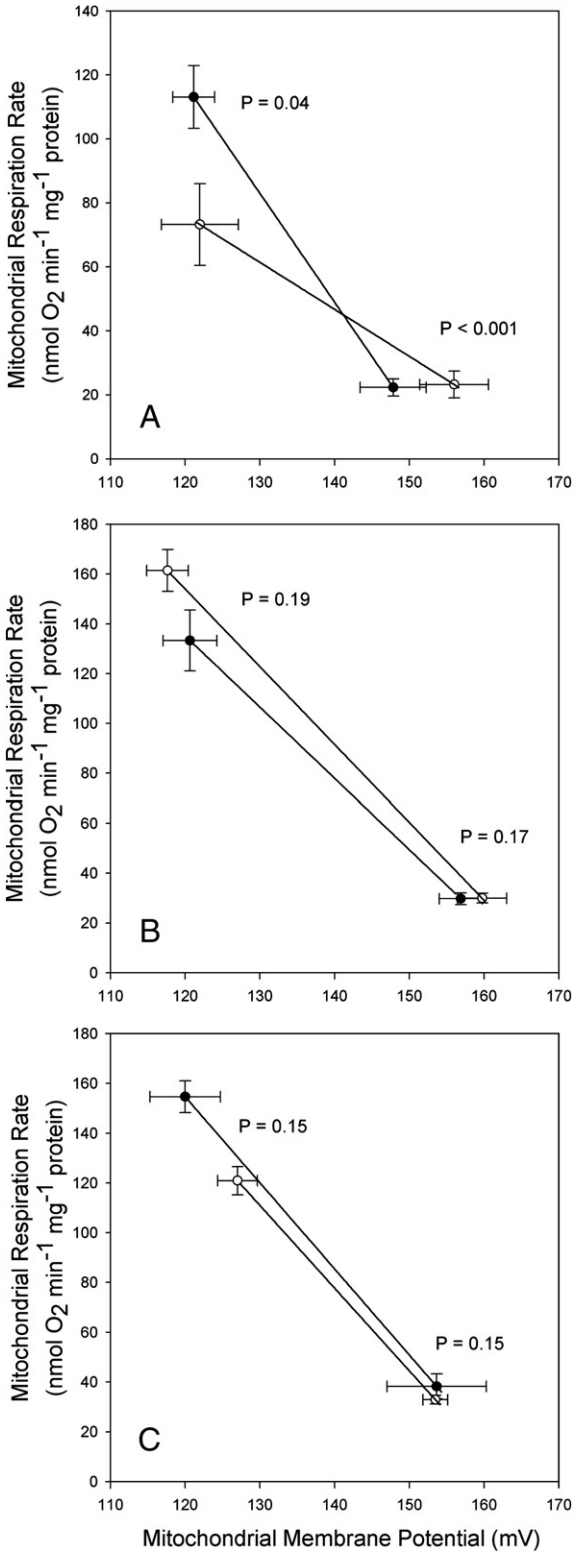

Fig. 3. Liver mitochondrial substrate oxidation kinetics measured in vitro at 37 °C. In each figure, substrate oxidation kinetics are shown for mitochondria from non-torpid (filled circles) and torpid (open circles) animals. The kinetics of substrate oxidation were not determined experimentally but, instead, were approximated as the linear relationship between state 3 (upper left) and state 4 (lower right) data points obtained from measurements of phosphorylation and proton leak kinetics, respectively. A. Balb/c mice. B. CD1 mice. C. C57/6N mice. Within each strain, differences between normothermia and torpor were determined by a Monte-Carlo method (see Section 2). Two *P*-values are presented, one for state 3 (upper left) and one for state 4 (lower right). All data are means ± SEM. $N = 8/8$ (normothermic/torpid) for Balb/c, $N = 9/12$ for CD1, and $N = 4/7$ for C57/6N.

On the whole, with succinate as substrate, both substrate oxidation and ADP phosphorylation were suppressed in Balb/c mice, whereas only ADP phosphorylation was suppressed in C57/6N mice, but to a considerable extent, although substrate oxidation was moderately suppressed when T_b was about 24 °C. By comparison in *P. sungorus* only substrate oxidation was suppressed, not ADP phosphorylation. Given that suppression of substrate oxidation in Balb/c mice reduces succinate-driven, but not glutamate-driven, respiration rate, it is likely that the site of inhibition is complex II, since this is unique to succinate oxidation. Complex II is a possible site of inhibition during torpor in *P. sungorus* [10] and is also suppressed during mammalian hibernation [40–42]. The site of inhibition of ADP phosphorylation in Balb/c and C57/6N is not known. Both ATP synthase and the adenine nucleotide translocator (ANT) are sites of inhibition of ADP phosphorylation during hibernation [43,44].

Regarding glutamate oxidation, in Balb/c mice, ADP phosphorylation was suppressed during torpor yet we observed no suppression of respiration rate. ADP phosphorylation had only 19–28% control of state 3 succinate-driven respiration (data not shown), and so the inhibition of ADP phosphorylation made a smaller contribution to the suppression of succinate oxidation rate than did the inhibition of complex II. Control of state 3 glutamate respiration rate in liver

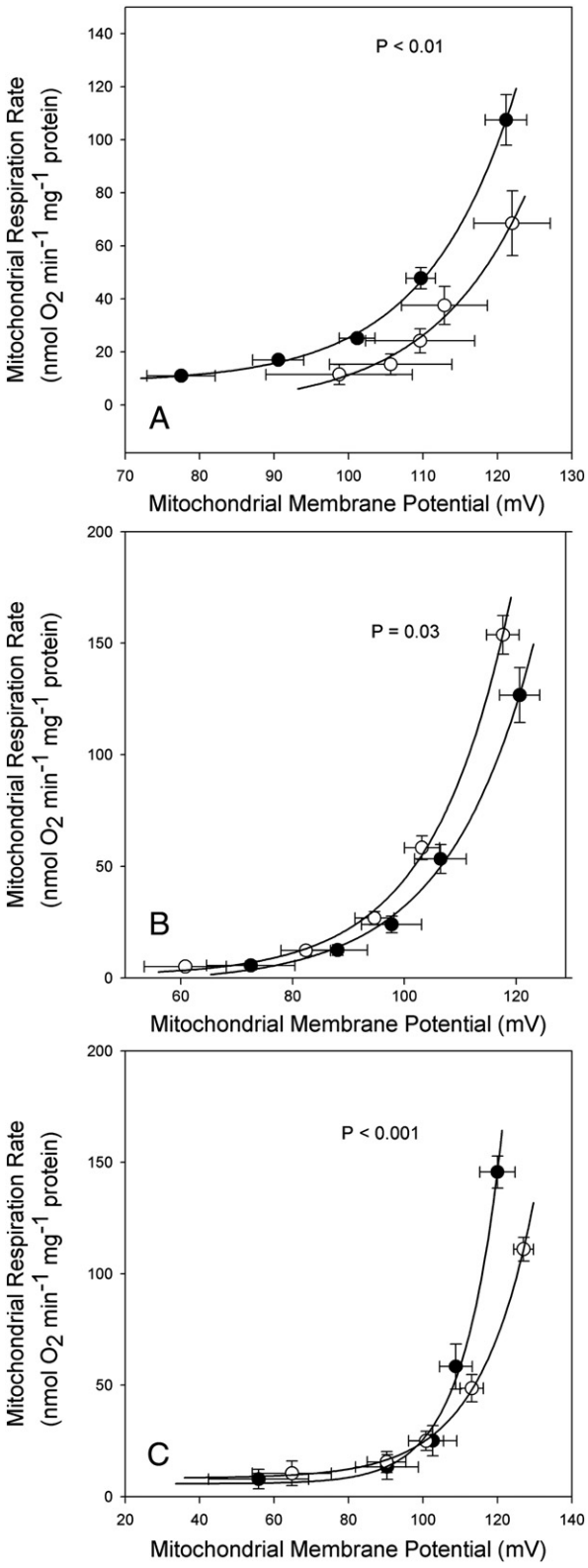

Fig. 4. Liver mitochondrial phosphorylation kinetics measured in vitro at 37 °C. In each figure, phosphorylation kinetics are shown for mitochondria from non-torpid (filled circles) and torpid (open circles) animals. For each kinetic curve, the uppermost data point represents state 3 respiration rate and membrane potential, and each subsequent data point results from stepwise inhibition of substrate oxidation using malonate, a competitive inhibitor of succinate dehydrogenase. A. Balb/c mice. B. CD1 mice. C. C57/6N mice. Within each strain, differences between normothermia and torpor were determined by a Monte-Carlo method (see Section 2). All data are means ± SEM. $N = 8/8$ (normothermic/torpid) for Balb/c, $N = 9/12$ for CD1, and $N = 4/7$ for C57/6N.

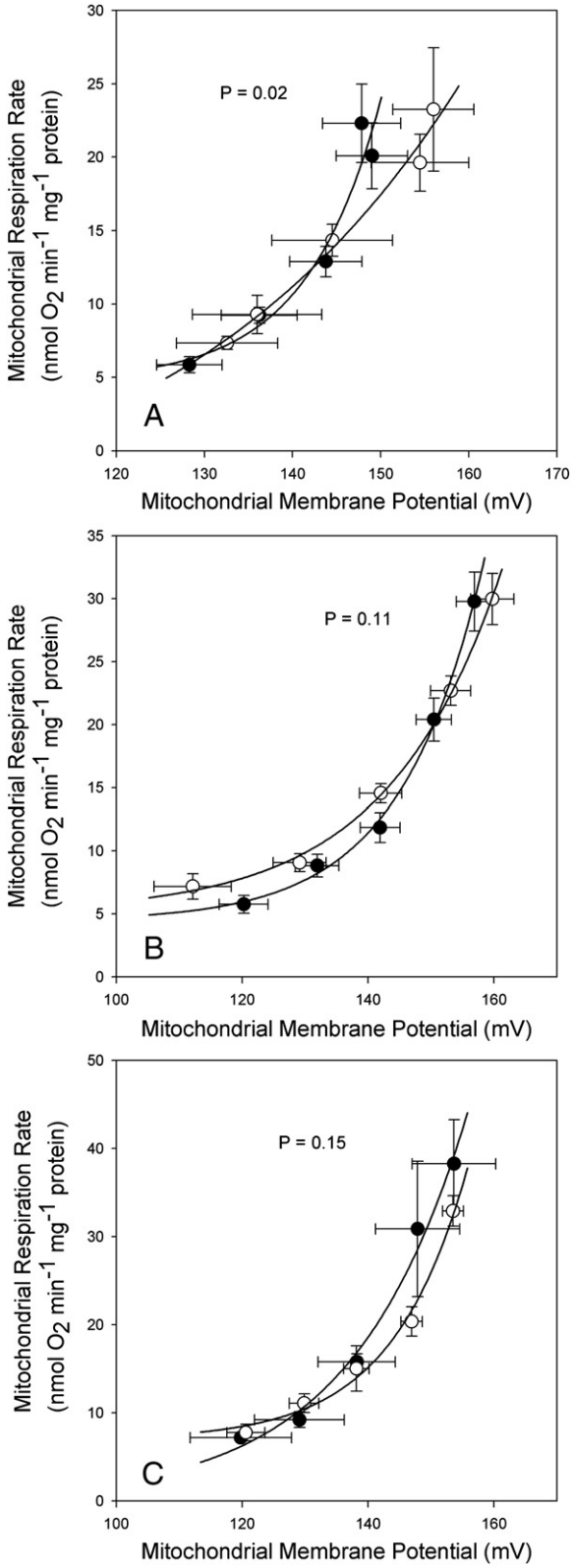

Fig. 5. Liver mitochondrial proton leak kinetics measured in vitro at 37 °C. In each figure, proton leak kinetics are shown for mitochondria from non-torpid (filled circles) and torpid (open circles) animals. For each kinetic curve, the uppermost data point represents state 4 respiration rate and membrane potential, and each subsequent data point results from stepwise inhibition of substrate oxidation using malonate, a competitive inhibitor of succinate dehydrogenase. A. Balb/c mice. B. CD1 mice. C. C57/6N mice. Within each strain, differences between non-torpid and torpid animals were determined by a Monte-Carlo method (see Section 2). All data are means ± SEM. $N = 8/8$ (normothermic/torpid) for Balb/c, $N = 9/12$ for CD1, and $N = 4/7$ for C57/6N.

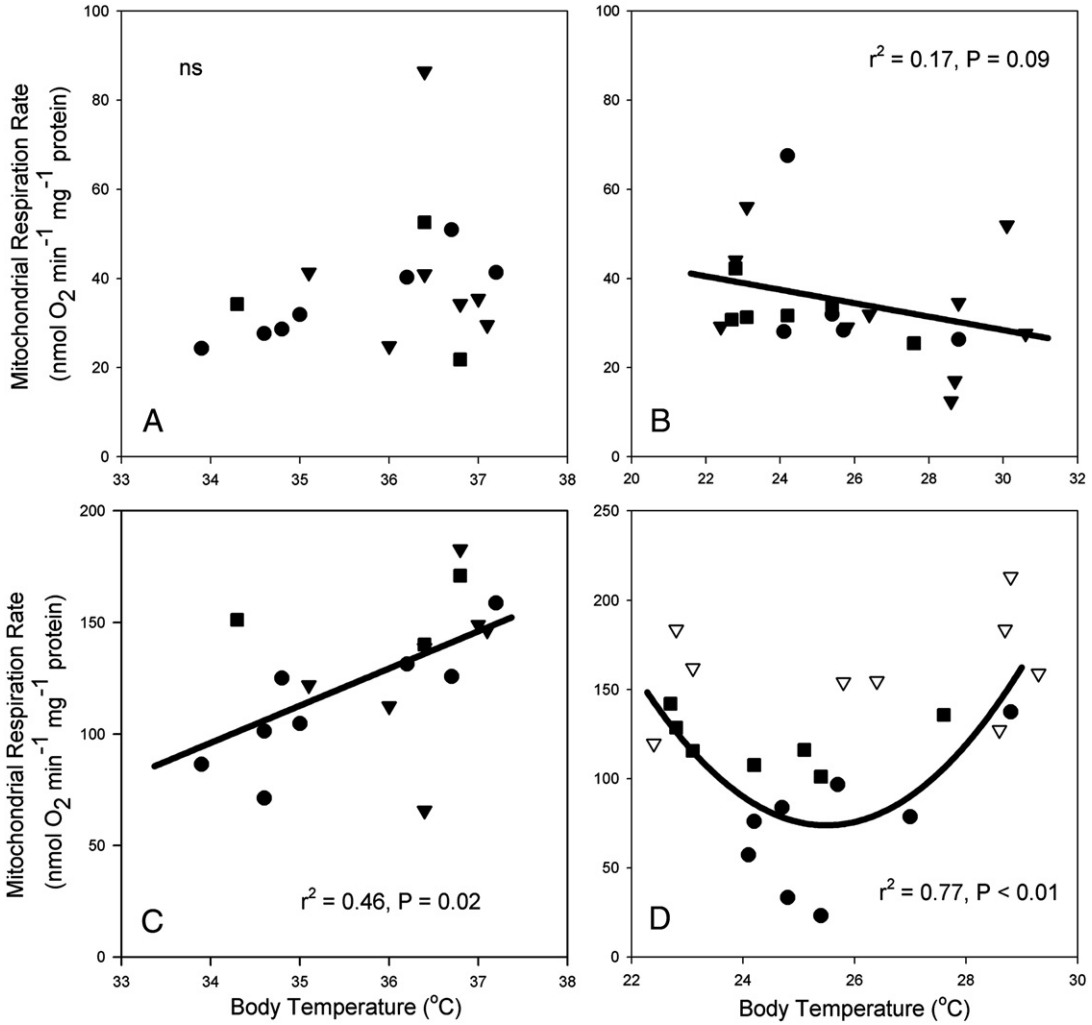

Fig. 6. Effect of body temperature (T_b) at time of sampling on non-torpid and torpid liver mitochondrial respiration rate (measured in vitro at 37 °C). A. Glutamate-driven state 3 respiration rate for mitochondria from non-torpid animals did not correlate with T_b. B. Glutamate-driven state 3 respiration rate for mitochondria from torpid animals may correlate negatively with T_b at sampling in all strains. C. Succinate-driven state 3 respiration rate for mitochondria from non-torpid animals correlated positively with T_b in all strains. D. Succinate-driven state 3 respiration rate for mitochondria from torpid animals showed a quadratic relationship with T_b at sampling in Balb/c and C57/6N mice but not CD1 mice.

mitochondria by ADP phosphorylation may be similar to that for succinate [32], so the lack of a corresponding suppression of substrate oxidation may prevent glutamate oxidation rate from being suppressed in this strain. By contrast, CD1 mice did not suppress succinate oxidation, yet glutamate oxidation rate was suppressed. This suggests that complex I, the glutamate transporters, and/or glutamate dehydrogenase (GDH) may be the site of mitochondrial suppression in CD1 mice. In *P. sungorus*, Heldmaier et al. [45] showed that GDH activity is not suppressed during torpor in any of several tissues examined (including liver). Finally, in C57/6N mice, the considerable reduction of ADP phosphorylation capacity could account for the suppression of glutamate-driven state 3 respiration rate in this strain, although we cannot rule out the possibility that some glutamate metabolism-specific component is also suppressed even if only transiently.

Thus, there are at least three sites of suppression of mitochondrial respiration during daily torpor in rodents: complex I, complex II, and some constituent of ADP phosphorylation. Which of these sites is suppressed, and to what extent, seems variable depending upon species (or method of torpor induction) and/or strain. Notwithstanding, the extent of MR suppression during torpor was the same for all strains of mice, and is comparable to the extent of MR suppression reported for *P. sungorus* [46]. Even if the torpor induction signals are the same in all strains, different mouse strains are known to react differently to the same molecular/physiological signals [47,48]. Moreover, it has been shown that torpor patterns differ significantly among species within the same genus (e.g. *Peromyscus*) even when held under the same conditions [49].

Suppression of liver mitochondrial metabolism during torpor is thought to contribute to the reduction of MR. Certainly, both parameters are lowered during daily torpor, but we cannot infer causation from these results. For torpid animals, we observed that liver mitochondrial respiration rate was more strongly correlated with T_b than with MR. In our previous study, active suppression of mitochondrial metabolism during torpor in *P. sungorus* was evident when measured in vitro at 37 °C or 30 °C, but not 23 °C or 15 °C [10]. Similarly, in the present study, there was evidence of active suppression of mitochondrial respiration rate during torpor in mice when measured at 37 °C but not 15 °C. Therefore, active mitochondrial suppression may be the predominant mechanism of MR suppression during torpor when T_b is high, whereas passive thermal effects may be the predominant mechanism when T_b is low. In

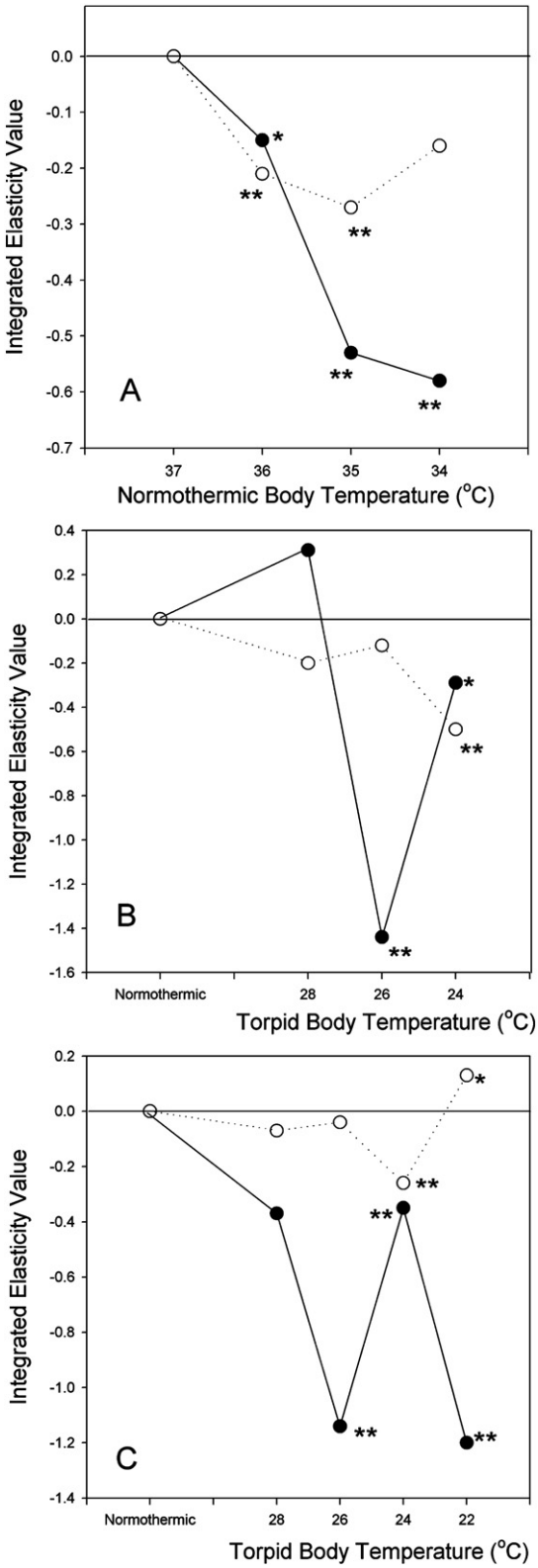

Fig. 7. Effect of body temperature (T_b) on the kinetics of ADP phosphorylation (closed circles) and substrate oxidation (open circles). Animals were grouped together into 1 °C (non-torpid animals) or 2 °C (torpid animals) T_b intervals so that T_b-related kinetic differences could be more readily assessed. A. Non-torpid animals for all strains were analyzed together, and animals with T_b approximating 37 °C were used as the control state. B. Torpid animals from Balb/c compared to non-torpid animals (used as the control state) from the same strain. C. Torpid animals from C57/6N compared to non-torpid animals (used as the control state) from the same strain. Kinetic differences were expressed as integrated elasticity values, which were statistically analyzed using a modified Monte-Carlo approach (see Section 2). $^{*}P<0.05$; $^{**}P<0.01$.

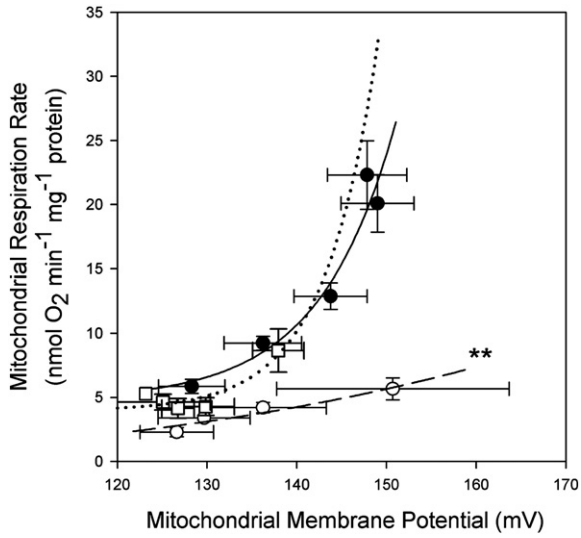

Fig. 8. Homeoconductivity of the inner mitochondrial membrane (IMM) during daily torpor in Balb/c mice. Compared to mitochondria from non-torpid animals measured at 37 °C (filled circles; solid line), the IMM proton conductance of mitochondria from non-torpid animals measured at 15 °C (open circles; dashed line) was significantly lower, whereas the IMM proton conductance of mitochondria from torpid animals measured at 15 °C (open squares; dashed line) was not different. Differences in proton leak kinetics between non-torpid mitochondria at 37 °C and the two other conditions were determined by Monte-Carlo analysis (see Section 2). Data are means ± SEM. For both normothermia and torpor, $N=8$ for 37 °C and $N=7$ for 15 °C.

support of this idea, with glutamate, torpid animals sampled at high T_b had lower mitochondrial respiration rates. With succinate, state 3 respiration rate was gradually reduced during torpor until T_b reached 25 °C, beyond which the inhibition was gradually reversed. Interestingly, the temperature at which succinate oxidation inhibition seems to begin reversing (i.e. 25 °C) corresponds to the range of temperatures (23–30 °C) over which active inhibition of succinate oxidation rate seemed to lose its impact on mitochondrial respiration rate in hamsters [10]. Since T_b remains highly regulated during torpor [50], it may be that regulation of liver mitochondrial oxidative capacity during torpor is somehow linked to T_b regulation. One possible benefit of this linked regulation is that the suppression of mitochondrial oxidative capacity could be reversed—in preparation of subsequent arousal—when T_b is low enough for passive thermal effects to suppress mitochondrial activity. The depression of liver mitochondrial activity likely contributes to lowering MR, but its correlation to MR may be weaker since liver accounts for only 15% of whole-animal basal metabolic rate [51] and MR can vary as a result of factors unrelated to liver mitochondrial activity or T_b, such as nest insulation, fur density, or patterns of peripheral blood flow.

The metabolic state transition between non-torpor and torpor, therefore, does not appear to follow a “switch” mechanism; rather, mitochondrial metabolism is gradually inhibited during torpor and then gradually reactivated again in preparation for arousal. A recent study of a hibernating rodent, *Ictidomys tridecemlineatus*, has shown similar findings: during arousal, liver mitochondrial respiration rate is gradually increased, and it does not reach levels comparable to summer active animals until the interbout euthermic phase, when T_b has returned to 37 °C [42]. These results are reminiscent of studies of the hypothalamic control of T_b during hibernation where the thermoregulatory setpoint is gradually lowered during entrance into hibernation, not immediately turned down to its lowest point [50]. Therefore, the transition out of, and presumably into, torpor is a gradual continuous process. Furthermore, the different sites of mitochondrial regulation may not be inhibited (or reactivated) synchronously during torpor; for example, in both Balb/c and C57 mice, ADP phosphorylation is inhibited at higher T_b than substrate

oxidation, and in C57 mice, substrate oxidation is reactivated while T_b is still low, but ADP phosphorylation is not.

4.2. Mitochondrial metabolism is occasionally suppressed in fasted, non-torpid mice

How much energy is saved by daily torpor is not entirely clear, and estimates range from 5% to 90% of daily energy expenditure [5,13,52]. Notwithstanding, daily torpor is undoubtedly part of the energy-saving strategy of fasted mice, who spent about 40% of their time torpid but were never torpid when fed. Energy savings could presumably be increased by longer and more frequent torpor bouts; however, torpor has costs [25,53], one of which is inactivity that precludes foraging. Fasting has been shown to increase diurnal activity levels in house mice, perhaps to facilitate increased foraging [54]. The average torpor bout length observed in this study (5.6 h) may represent a balance between energy savings and the need to forage.

Moderate reductions in T_b and MR during periods of non-torpor in fasted animals could conserve additional energy while permitting activity and foraging. Non-torpid animals displayed considerable variation in T_b and MR, sometimes reducing T_b as low as 34 °C, with a corresponding reduction of MR up to 25%. By comparison, fed animals rarely had T_b less than 36 °C at the same time of day. When T_b and MR were reduced, state 3 respiration was also reduced (although the suppression was not statistically significant for glutamate). Therefore, non-torpid fasted animals periodically reduced mitochondrial respiratory capacity—albeit to a lesser extent than during torpor—in order to further reduce their energy demands. Within non-torpid animals, changes in liver mitochondrial succinate oxidation rate did correlate with changes in MR, which provides better evidence to support the idea that suppressing liver mitochondrial activity can bring about MR suppression.

4.3. Homeoconductivity of mitochondrial inner membrane during daily torpor may alleviate ROS production

It has been suggested that decreased IMM proton leakiness during torpor could save energy [12]. Although proton leakiness may not be actively reduced during hibernation [55], except at high or low levels of dietary linoleic acid [27], low temperature passively lowers mitochondrial proton conductance [34,56], and so proton leakiness may, in fact, be lower during hibernation, though measurements at hibernation-like temperatures are lacking. By contrast, in both mice (this study) and hamsters [10], we have observed that IMM proton conductance was about 2-fold higher in mitochondria from torpid animals compared to non-torpid animals when measured at 15 °C (the lower limit of torpid T_b). As a result, it was not different from IMM proton conductance of mitochondria from non-torpid animals measured at 37 °C (i.e., "homeoconductivity", the maintenance of constant IMM proton conductivity despite large temperature changes) [57]. We should point out that, because we did not use nigericin, our measurements of proton leak kinetics assume that ΔpH is constant between 37 °C and 15 °C—which has been shown previously by Dufour et al. [34] in rat liver mitochondria—and between metabolic states. In order for the observed difference in proton leakiness between non-torpid and torpid animals at 15 °C to be eliminated, ΔpH would have to be 20 mV higher in torpid animals than non-torpid animals. Given that ΔpH is about 30–50 mV in rat liver mitochondria [58], a 40–70% change in ΔpH between metabolic states would be required to eliminate our observed difference. Since other studies showing changes in mitochondrial respiration rate between experimental conditions have shown only negligible changes in ΔpH at best [35,36], this seems unlikely.

There is also evidence that mechanisms of altering proton leak during torpor may differ between these two species. For example, in torpid hamsters, proton leakiness is increased regardless of assay temperature, whereas in torpid mice, it is lower than non-torpid fasted animals when measured at 37 °C but higher when measured at 15 °C. Since we included BSA in our assay buffer, which binds free fatty acids (FFA), any proton leak mechanisms that require FFA cannot be responsible for this homeoconductivity. Several fatty acid-independent factors can alter IMM proton leakiness, particularly changes in IMM proton permeability via changes in IMM surface area or IMM phospholipid composition [59], and ANT content [60]. We have previously shown that ANT content does not increase during daily torpor in *P. sungorus* [10], but, to our knowledge, there are no studies of mitochondrial phospholipid composition or IMM surface area during daily torpor. IMM surface area has been shown to increase during hibernation [61], but no consistent changes in IMM phospholipid composition during hibernation have been reported [62]. We have not explored the mechanisms responsible for homeoconductivity, but our data do suggest a possible physiological consequence. In both hamsters and mice, because substrate oxidation was significantly reduced (actively and/or passively) during torpor at 15 °C, the increased proton leakiness caused $\Delta\Psi_m$ to be more than 10 mV lower during daily torpor. Increased IMM proton leakiness has been shown to correspond with decreased ROS production [63–65], so homeoconductivity may alleviate oxidative stress during torpor more than would be predicted based simply on lower oxygen consumption rates, given that small changes in $\Delta\Psi_m$ can have disproportionately large impacts on ROS production rates [66]. We are currently pursuing measurements of the effect of torpor on mitochondrial ROS production to test this hypothesis.

4.4. Perspectives and significance

Much of the research about daily torpor in fasted animals, including house mice, has focused on the environmental cues and/or endogenous molecular signals that are necessary to bring about the expression of daily torpor. The ultimate downstream targets of these molecular signals—directly responsible for the depression of MR that characterizes daily torpor—have been comparatively ignored, and this study helps to fill this gap. We have identified at least three mitochondrial sites that may be downregulated in liver mitochondria during daily torpor in mice: complex I, complex II, and ADP phosphorylation. Leptin administration in *ob*/*ob* mice has been shown to upregulate several enzymes involved in ETC electron transport in liver [67], including subunits of NADH dehydrogenase and ATP synthase, as well as ANT2 and the dicarboxylate transporter. The decline in leptin during fasting-induced torpor, therefore, could bring about downregulation of these same enzymes, contributing to the mitochondrial suppression seen here. Furthermore, basal IMM proton leakiness is higher in *ob*/*ob* mice [68], so declining leptin levels could account for the homeoconductivity of torpid mice seen here. How the other molecular signals thought to be involved in the induction of fasting-induced torpor may reduce mitochondrial metabolism is less clear. As we continue to identify sites that are downregulated during bouts of torpor, we may be able to use our existing understanding of the regulation of these sites in a bottom-up approach to further elucidate the torpor induction pathway from its beginning to its end.

Acknowledgements

Financial support for this work came from the Natural Sciences and Engineering Research Council of Canada in the form of a Postgraduate Scholarship (JCLB), a Discovery Grant (JFS), and Research Tools and Infrastructure Grant (JFS).

References

[1] D.R. Reed, A.A. Bachmanov, M.G. Tordoff, Forty mouse strain survey of body composition, Physiol. Behav. 91 (2007) 593–600.
[2] F.H. Bronson, Susceptibility of the fat reserves of mice to natural challenges, J. Comp. Physiol. B 157 (1987) 551–554.
[3] F.H. Bronson, P.D. Heideman, M.C. Kerbeshian, Lability of fat stores in peripubertal wild house mouse, J. Comp. Physiol. B 161 (1991) 15–18.
[4] J.W. Hudson, I.M. Scott, Daily torpor in the laboratory mouse, *Mus musculus var. albino*, Physiol. Zool. 52 (1978) 205–218.
[5] F. Geiser, Metabolic rate and body temperature reduction during hibernation and daily torpor, Annu. Rev. Physiol. 66 (2004) 239–274.
[6] J. Dark, D.R. Miller, P. Licht, I. Zucker, Glucoprivation couteracts effects of testosterone on daily torpor in Siberian hamsters, Am. J. Physiol., Regul. Integr. Comp. Physiol. 270 (1996) R398–R403.
[7] F. Geiser, Reduction of metabolism during hibernation and daily torpor in mammals and birds: temperature effect or physiological inhibition? J. Comp. Physiol. B 158 (1988) 25–37.
[8] M. Guppy, P. Withers, Metabolic depression in animals: physiological perspectives and biochemical generalizations, Biol. Rev. 74 (1999) 1–40.
[9] D.F.S. Rolfe, G.C. Brown, Cellular energy utilization and molecular origin of standard metabolic rate in mammals, Physiol. Rev. 77 (1997) 731–758.
[10] J.C.L. Brown, A.R. Gerson, J.F. Staples, Mitochondrial metabolism during daily torpor in the dwarf Siberian hamster: role of active inhibition and passive thermal effects, Am. J. Physiol., Regul. Integr. Comp. Physiol. 293 (2007) R1833–R1845.
[11] M.B. Diaz, M. Lange, G. Heldmaier, M. Klingenspor, Depression of transcription and translation during daily torpor in the Djungarian hamster (*Phodopus sungorus*), J. Comp. Physiol. B 174 (2004) 495–502.
[12] S.L. Martin, G.D. Maniero, C. Carey, S.C. Hand, Reversible depression of oxygen consumption in isolated liver mitochondria during hibernation, Physiol. Biochem. Zool. 72 (1999) 255–264.
[13] G. Heldmaier, S. Steinlechner, Seasonal pattern and energetics of short daily torpor in the Djungarian hamster, *Phodopus sungorus*, Oecologia 48 (1981) 265–270.
[14] G. Heldmaier, S. Steinlechner, Seasonal control of energy requirements for thermoregulation in the Djungarian hamster (*Phodopus sungorus*), living in natural photoperiod, J. Comp. Physiol. B 142 (1981) 429–437.
[15] T. Ruf, S. Steinlechner, G. Heldmaier, Rhythmicity of body temperature and torpor in the Djungarian hamster, *Phodopus sungorus*, in: A. Malan, B. Canguilhem (Eds.), Living in the Cold: 2nd International Symposium, John Libbey Eurotext, London, 1989, pp. 53–61.
[16] N.F. Ruby, N. Ibuka, B.M. Barnes, I. Zucker, Suprachiasmatic nuclei influence torpor and circadian temperature rhythms in hamsters, Am. J. Physiol., Regul. Integr. Comp. Physiol. 257 (1989) R210–R215.
[17] P.M. Vitale, J.M. Darrow, M.J. Duncan, C.A. Shustak, B.D. Goldman, Effects of photoperiod, pinealectomy and castration on body weight and daily torpor in Djungarian hamsters (*Phodopus sungorus*), J. Endocrinol. 106 (1985) 367–375.
[18] N.F. Ruby, R.J. Nelson, P. Licht, I. Zucker, Prolactin and testosterone inhibit torpor in Siberian hamsters, Am. J. Physiol., Regul. Integr. Comp. Physiol. 264 (1993) R123–R128.
[19] D.A. Freeman, D.A. Lewis, A.S. Kauffman, R.M. Blum, J. Dark, Reduced leptin concentrations are permissive for display of torpor in Siberian hamsters, Am. J. Physiol., Regul. Integr. Comp. Physiol. 287 (2004) R97–R103.
[20] G.P. Webb, S.A. Jagot, M.E. Jakobson, Fasting-induced torpor in *Mus musculus* and its implications in the use of murine models for human obesity studies, Comp. Biochem. Physiol. A 72 (1982) 211–219.
[21] F. Geiser, B.M. McAllan, G.J. Kenagy, S.M. Hiebert, Photoperiod affects daily torpor and tissue fatty acid composition in deer mice, Naturwissenschaften 94 (2007) 319–325.
[22] S.J. Swoap, The pharmacology and molecular mechanisms underlying temperature regulation and torpor, Biochem. Pharmcol. 76 (2008) 817–824.
[23] T. Ruf, A. Stieglitz, S. Steinlechner, J.L. Blank, G. Heldmaier, Cold exposure and food restriction facilitate physiological responses to short photoperiod in Djungarian hamsters (*Phodopus sungorus*), J. Exp. Zool. 267 (1993) 104–112.
[24] N.F. Ruby, I. Zucker, Daily torpor in the absence of the suprachiasmatic nucleus in Siberian hamsters, Am. J. Physiol., Regul. Integr. Comp. Physiol. 263 (1992) R353–R362.
[25] M.S. Wojciechowski, M. Jefimow, Is torpor only an advantage? Effect of thermal environment on torpor use in the Siberian hamsters (*Phodopus sungorus*), J. Physiol. Pharmacol. 57 (2006) 83–92.
[26] C.L. Frank, The influence of dietary fatty acids on hibernation by golden-mantled ground squirrels (*Spermophilus lateralis*), Physiol. Zool. 65 (1992) 906–920.
[27] A.R. Gerson, J.C.L. Brown, R. Thomas, M.A. Bernards, J.F. Staples, Effects of dietary polyunsaturated fatty acids on mitochondrial metabolism in mammalian hibernation, J. Exp. Biol. 211 (2008) 2689–2699.
[28] S.M. Hiebert, E.K. Fulkerson, K.T. Lindermayer, S.D. McClure, Effect of temperature on preference for dietary unsaturated fatty acids in the Djungarian hamster (*Phodopus sungorus*), Can. J. Zool. 78 (2000) 1361–1368.
[29] H.M. Muleme, A.C. Walpole, J.F. Staples, Mitochondrial metabolism in hibernation: metabolic suppression, temperature effects, and substrate preferences, Physiol. Biochem. Zool. 79 (2006) 474–483.
[30] M. Takaki, H. Nakahara, Y. Kawatani, K. Utsumi, H. Suga, No suppression of respiratory function of mitochondria isolated from the hearts of anesthetized rats with high-dose pentobarbital sodium, Jpn. J. Physiol. 47 (1997) 87–92.
[31] H. Rottenberg, Membrane potential and surface potential in mitochondria: uptake and binding of lipophilic cations, J. Membr. Biol. 81 (1984) 127–138.
[32] M.D. Brand, M.-E. Harper, H.C. Taylor, Control of the effective P/O ratio of oxidative phosphorylation in liver mitochondria and hepatocytes, Biochem. J. 291 (1993) 739–748.
[33] D.F.S. Rolfe, A.J. Hulbert, M.D. Brand, Characteristics of mitochondrial proton leak and control of oxidative phosphorylation in the major oxygen-consuming tissues of the rat, Biochim. Biophys. Acta 1118 (1994) 405–416.
[34] S. Dufour, N. Rousse, P. Canioni, P. Diolez, Top-down control analysis of temperature effect on oxidative phosphorylation, Biochem. J. 314 (1996) 743–751.
[35] N.I. Kavanagh, E.K. Ainscow, M.D. Brand, Calcium regulation of oxidative phosphorylation in rat skeletal muscle mitochondria, Biochim. Biophys. Acta 1457 (2000) 57–70.
[36] A. Marcinkeviciute, V. Mildaziene, S. Crumm, O. Demin, J.B. Hoek, B. Kholodenko, Kinetics and control of oxidative phosphorylation in rat liver mitochondria after chronic ethanol feeding, Biochem. J. 349 (2000) 519–526.
[37] E.K. Ainscow, M.D. Brand, Errors associated with metabolic control analysis: application of Monte-Carlo simulation of experimental data, J. Theor. Biol. 194 (1998) 223–233.
[38] E.K. Ainscow, M.D. Brand, The responses of rat hepatocytes to glucagon and adrenaline: application of quantified elasticity analysis, Eur. J. Biochem. 265 (1999) 1043–1055.
[39] M. Sokolovic, A. Sokolovic, D. Wehkamp, E.V.L. van Themaat, D.R. de Waart, L.A. Gilhuijs-Pederson, Y. Nikolsky, A.H.C. van Kampen, T.B.M. Hakvoort, W.H. Lamers, Fasting induces a biphasic metabolic response in murine small intestine, BMC Genomics 9 (2007) 528–547.
[40] S.C. Gehnrich, J.R. Aprille, Hepatic gluconeogenesis and mitochondrial function during hibernation, Comp. Biochem. Physiol. B 91 (1988) 11–16.
[41] N.J. Fedotcheva, A.A. Sharyshev, G.D. Mironova, M.N. Kondrashova, Inhibition of succinate oxidation and K^+ transport in mitochondria during hibernation, Biochem. Physiol. B 82 (1985) 191–195.
[42] C. Armstrong, J. Staples, The role of succinate dehydrogenase and oxaloacetate in metabolic suppression during hibernation and arousal, J. Comp. Physiol. B (in press).
[43] G.E. Bronnikov, S.O. Vingradova, V.S. Mezentseva, Changes in kinetics of ATP-synthase and in concentrations of adenine nucleotides in ground squirrel liver mitochondria during hibernation, Comp. Biochem. Physiol. B 97 (1990) 411–415.
[44] Z.G. Amerkhanov, M.V. Yegorova, O.V. Markova, E.N. Mokhova, Carboxyatractylate- and cyclosporin A-sensitive uncoupling in liver mitochondria of ground squirrels during hibernation and arousal, Biochem. Mol. Biol. Int. 38 (1996) 863–870.
[45] G. Heldmaier, M. Klingenspor, M. Werneyer, B.J. Lampi, S.P. Brooks, K.B. Storey, Metabolic adjustments during daily torpor in the Djungarian hamster, Am. J. Physiol. 276 (1999) E896–906.
[46] R. Kirsch, A. Ouarour, P. Pevet, Daily torpor in the Djungarian hamster (*Phodopus sungorus*): photoperiodic regulation, characteristics and circadian organization, J. Comp. Physiol. A 168 (1991) 121–128.
[47] M.J. Marks, J.B. Burch, A.C. Collins, Genetics of nicotine response in four inbred strains of mice, J. Pharmacol. Exp. Ther. 226 (1983) 291–302.
[48] A. Funkat, C.M. Massa, Y. Jovanovska, J. Proietto, S. Andrikopoulos, Metabolic adaptations of three inbred strains of mice (C57/6NBL/6, DBA/2, and 129T2) in response to a high-fat diet, J. Nutr. 134 (2004) 3264–3269.
[49] M.G. Tannenbaum, E.B. Pivorum, Differences in daily torpor patterns among three southeastern species of *Peromyscus*, J. Comp. Physiol. B 154 (1984) 233–236.
[50] H.C. Heller, G.W. Colliver, CNS regulation of body temperature during hibernation, Am. J. Physiol. 227 (1974) 583–589.
[51] A.W. Martin, F.A. Fuhrman, The relationship between summated tissue respiration and metabolic rate in the mouse and dog, Physiol. Zool. 28 (1955) 18–34.
[52] S. Ortmann, G. Heldmaier, J. Schmid, J.U. Ganzhorn, Spontaneous daily torpor in Malagasy mouse lemurs, Naturwissenschaften 84 (1997) 28–32.
[53] T. Deboer, I. Tobler, Sleep EEG after daily torpor in the Djungarian hamster: similarity to the effects of sleep deprivation, Neurosci. Lett. 166 (1994) 35–38.
[54] J.M. Overton, T.D. Williams, Behavioral and physiologic responses to calorie restriction in mice, Physiol. Behav. 81 (2004) 749–754.
[55] J.L. Barger, M.D. Brand, B.M. Barnes, B.B. Boyer, Tissue-specific depression of mitochondrial proton leak and substrate oxidation in hibernating arctic ground squirrels, Am. J. Physiol., Regul. Integr. Comp. Physiol. 284 (2003) R1306–1313.
[56] M.E. Chamberlain, Top-down control analysis of the effect of temperature on ectotherm oxidative phosphoryaltion, Am. J. Physiol., Regul. Integr. Comp. Physiol. 287 (2004) R794–R800.
[57] J. Staples, A. Gerson, J. Brown, Mitochondrial respiration and proton leak in hibernation and daily torpor, in: B.G. Lovegrove, A.E. McKechnie (Eds.), Hypometabolism in Animals: Hibernation, Torpor, and Cryobiology, Interpak Books, Pietermaritzburg, 2008, pp. 65–74.
[58] A. Devin, B. Guerin, M. Rigoulet, Response of isolated rat liver mitochondria to variation of external osmolarity in KCl medium: regulation of matrix volume and oxidative phosphorylation, J. Bioenerg. Biomembr. 29 (1997) 579–590.
[59] M.D. Brand, L.F. Chien, E.K. Ainscow, D.F. Rolfe, R.K. Porter, The causes and functions of mitochondrial proton leak, Biochim. Biophys. Acta 1187 (1994) 132–139.
[60] M.D. Brand, J.L. Pakay, A. Ocloo, J. Kokoszka, D.C. Wallace, P.S. Brookes, E.J. Cornwall, The basal proton conductance of mitochondria depends on adenine nucleotide translocase content, Biochem. J. 392 (2005) 353–362.
[61] M. Malatesta, S. Battistelli, M.B.L. Rocchi, C. Zancanaro, S. Fakan, G. Gazzanelli, Fine structural modifications of liver, pancreas and brown adipose tissue mitochondria from hibernating, arousing and euthermic dormice, Cell Biol. Int. 25 (2001) 131–138.
[62] H.V. Carey, M.T. Andrews, S.L. Martin, Mammalian hibernation: cellular and molecular responses to depressed metabolism and low temperature, Physiol. Rev. 83 (2003) 1153–1181.

[63] P.S. Brookes, Mitochondrial H^+ leak and ROS generation: an odd couple, Free Radic. Biol. Med. 38 (2005) 12–23.
[64] J.R. Speakman, D.A. Talbot, C. Selman, S. Snart, J.S. McLaren, P. Redman, E. Krol, D.M. Jackson, M.S. Johnson, M.D. Brand, Uncoupled and surviving: individual mice with high metabolism have greater mitochondrial uncoupling and live longer, Aging Cell 3 (2004) 87–95.
[65] Y.-W.C. Fridell, A. Sanchez-Blanco, B.A. Silvia, S.L. Helfand, Targeted expression of the human uncoupling protein 2 (hUCP2) to adult neurons extends life span in the fly, Cell Metab. 1 (2005) 145–152.
[66] S. Miwa, M.D. Brand, Mitochondrial matrix reactive oxygen species production is very sensitive to mild uncoupling, Biochem. Soc. Trans. 31 (2003) 1300–1301.
[67] C.-P. Liang, A.R. Tall, Transcriptional profiling reveals global defects in energy metabolism, lipoprotein, and bile acid synthesis and transport with reversal by leptin treatment in *ob*/*ob* mouse liver, J. Biol. Chem. 276 (2001) 49066–49076.
[68] R.K. Porter, J.F. Andrews, Effects of leptin on mitochondrial 'proton leak' and uncoupling proteins: implications for mammalian energy metabolism, Proc. Nutr. Soc. 57 (1998) 455–460.